The Astrophysical Journal, 750:50 (7pp), 2012 May 1 doi:10.1088/0004-637X/750/1/50

EVIDENCE FOR POLAR X-RAY JETS AS SOURCES OF MICROSTREAM PEAKS IN THE SOLAR WIND

Marcia Neugebauer
Lunar and Planetary Laboratory, University of Arizona, Tucson, AZ 85721, USA; mneugeb@lpl.arizona.edu
Received 2011 August 7; accepted 2012 January 10; published 2012 April 13

ABSTRACT

It is proposed that the interplanetary manifestations of X-ray jets observed in solar polar coronal holes during periods of low solar activity are the peaks of the so-called microstreams observed in the fast polar solar wind. These microstreams exhibit velocity fluctuations of ± 35 km s^{-1}, higher kinetic temperatures, slightly higher proton fluxes, and slightly higher abundances of the low-first-ionization-potential element iron relative to oxygen ions than the average polar wind. Those properties can all be explained if the fast microstreams result from the magnetic reconnection of bright-point loops, which leads to X-ray jets which, in turn, result in solar polar plumes. Because most of the microstream peaks are bounded by discontinuities of solar origin, jets are favored over plumes for the majority of the microstream peaks.

Key words: solar wind – Sun: X-rays, gamma rays

1. INTRODUCTION

Although the fast polar solar wind has much less structure than the slow wind (Bame et al. 1977), it is not totally uniform, but exhibits some structures that are probably of solar origin. Such structures include occasional coronal mass ejections (Gosling et al. 1998), large amplitude Alfvén waves, pressure-balance structures (Thieme et al. 1990; McComas et al. 1996), and features called microstreams (Neugebauer et al. 1995). The purpose of this paper is to present further arguments to support a connection between X-ray jets or plumes in polar coronal holes and the microstreams. Section 2 reviews some relevant observations of jets and plumes. Section 3 reviews previous work on microstreams and presents new analyses to support the connection to jets. Section 4 presents conclusions and discussion.

2. JETS AND PLUMES

Observations of hot X-ray jets by the *Yohkoh* and *Hinode* spacecraft have provided a great deal of insight into their origin and properties (see, e.g., references in Cirtain et al. 2007, and Moreno-Insertis et al. 2008). It is generally agreed that jets are formed by the reconnection of newly emerging bright-point loops with previously open magnetic fields (e.g., Subramanian et al. 2010). Some of the relevant properties of the jets are listed in Table 1. They appear episodically in the chromospheric network as dense, hot, fast plasma channeled along magnetic field lines. A jet typically lasts for a few to tens of minutes, and there may be multiple outbursts during that time (Madjarska 2011). They typically have sharp edges defining structures with widths of $\sim 10^4$ km.

Polar plumes have long been studied in white light and other wavelengths; see references in the review of coronal holes by Cranmer (2009). Like the jets, they arise from the chromospheric network and are episodic, lasting on the order of a day and recurring intermittently over a few weeks. They are wider ($(2\text{–}4) \times 10^4$ km) and have less distinct or fuzzier edges than jets. They are denser and cooler than the interplume plasma. At low solar altitudes, most reports say that the plasma is slower than the surrounding corona with the speed increasing with increasing height, but the EUV observations by Gabriel et al. (2003) between 1.05 and 1.35 solar radii show the plume flow speed exceeding that of the interplume plasma. The properties of plumes are compared to those of jets in Table 1.

Raouafi et al. (2008) have shown that polar X-ray jets are precursors of polar plumes. Jets sometimes also enhance the brightness of existing plumes.

It is well established that, relative to the photosphere, the material in plumes is enhanced in elements with low first-ionization potential (FIP) (Wilhelm 2006). Low-FIP elements are also enhanced in bright-point loops (Subramanian et al., 2010). The elemental composition of X-ray jets has not been reported. It is logical to assume, however, that if the jets come from bright-point eruptions and evolve into plumes, they are also enhanced in low-FIP elements.

3. SOLAR WIND

There is some disagreement about the contribution of jets and plumes to the fast polar solar wind. Some solar physicists have argued that plumes are a major contributor (e.g., Gabriel et al. 2003), and others believe they make only a minor, if any, contribution (e.g., Wang et al. 1998; Von Steiger et al. 1999; Wilhelm et al. 2000; Wilhelm 2006; Subramanian et al. 2010). If plumes do feed material into the wind, there is further disagreement about whether the plume material retains its identity (e.g., Thieme et al. 1990; Neugebauer et al. 1995; Reisenfeld et al. 1999; Velli et al. 2011) or is mixed in with the interplume plasma so its source is no longer identifiable (Suess 1998).

Neugebauer et al. (1995, hereafter Paper 1) studied the properties of velocity fluctuations in the high-speed wind when *Ulysses* was in the flow from the southern polar coronal hole at latitudes of $-60°$ to $-80°$ in 1994. The results of that study can be summarized as follows. (1) The velocity variations were not random, but organized into structures called "microstreams" with amplitudes of ± 25 km s^{-1}. (2) The mean half-width of the microstreams was 0.4 days. (3) The microstreams recurred on timescales of 2–3 days, with spectral peaks at 1.9 and 3.3 days. (4) The proton kinetic temperature variations were positively correlated with the speed variations; i.e., the faster plasma was hotter than the slower plasma. (5) The density and temperature profiles showed the expected signatures of

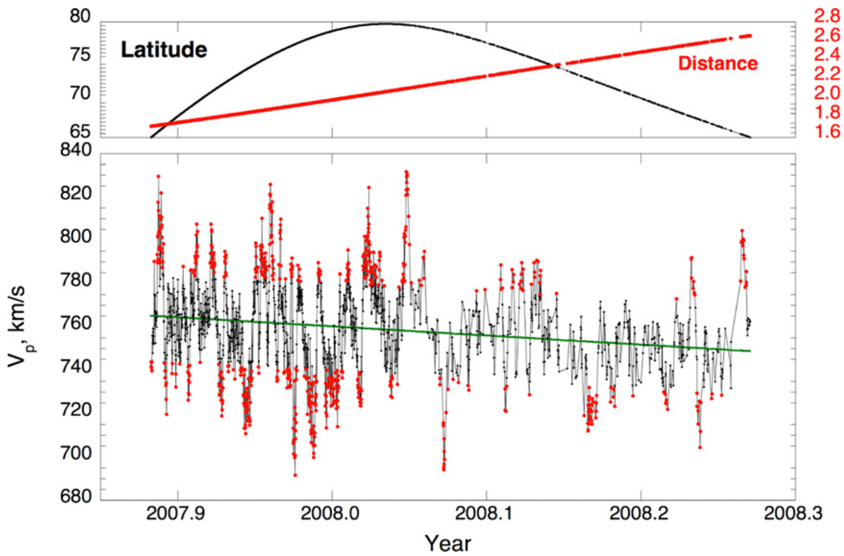

Figure 1. Top: heliographic latitude (black, in degrees) and distance (red, in AU) of the *Ulysses* spacecraft vs. year. Bottom: hourly averages of proton speed vs. year. The green line is the average speed during the interval and the red symbols mark hours for which the speeds were more than 20 km s^{-1} above or below the average.

Table 1
Some Similarities and Differences between X-Ray Jets and Polar Coronal Plumes

Jets	Plumes
Episodic	Episodic
Minutes to tens of minutes	~1 day
Arise from network	Arise from network
Denser than interplume	Denser than interplume
Hotter than interplume	Cooler than interplume
Faster than interplume	± interplume
Sharp edges	Indistinct edges
10^4 km wide	(2–4) × 10^4 km wide
Probable enhanced low FIP	Enhanced low FIP

pileup on positive velocity gradients and expansion when the velocity was decreasing. (6) The faster flows had greater alpha-particle abundance than did the slower flows. (7) The absence of a latitude dependence of either the temporal duration at the spacecraft or the recurrence rate of the microstreams suggested that the microstreams were caused by temporal rather than by quasistationary (greater than a few days) spatial variations in the solar source.

This paper augments the analysis in Paper 1 by considering data from the *Ulysses* north polar passage during late 2007 and early 2008, when solar activity was exceptionally low. The top panel of Figure 1 presents the heliographic latitude and solar radial distance of the *Ulysses* spacecraft versus fractional year during the north polar passage under investigation herein. The bottom panel shows hourly averages of the speed of solar-wind protons as measured by the SWOOPS instrument (Bame et al. 1992). A linear fit of speed versus time (or, nearly equivalently, speed versus solar distance) is indicated by the green line. The red dots indicate those hours during which the speed was 20 km s^{-1} greater than or less than the average speed indicated by the green line. Tracking of the *Ulysses* spacecraft was continuous until the maximum 80° latitude was reached, after which there were gaps in the data. Periods when the speed was more than 20 km s^{-1} from the mean (i.e., those with red dots in Figure 1) for at least six consecutive hours were selected for analysis. There were 18 such high-speed intervals, called "Peaks," and 16 low-speed intervals, called "Dips."

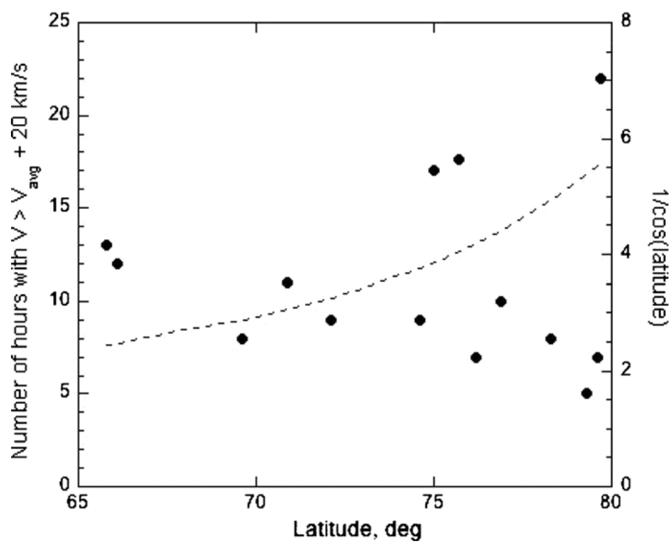

Figure 2. Points, scale on the left: the number of hours that the velocity in a Peak exceeded the average speed +20 km s^{-1}. Dashed line, scale on the right: $1/\cos$(latitude).

The magnetic fields in the polar coronal holes during the 2007–2008 solar minimum were weaker than they were during the previous minimum. Similar microstreams were observed, but was their thickness still independent of solar latitude? If microstream peaks were long-lived compared to their observed durations and had a uniform thickness throughout the polar region, the time required for each of them to corotate past the spacraft should increase with latitude λ as $1/\cos\lambda$. At the extreme, a stationary structure located at the pole would be observed continuously by a spacecraft right over the pole. Figure 2 tests whether, as before, the 2007–2008 microstreams were episodic or quasistationary. The points in Figure 2 show the number of hours that the speed in each of the Peaks exceeded the average speed +20 km s^{-1} plotted versus heliographic latitude λ. Data are included in Figure 2 through 2008 January 13, when the telemetry coverage was still complete. The dashed line in Figure 2 is $1/\cos\lambda$. A fit to the points shows a very weak negative correlation between width and latitude (coefficent $R = -0.03$) rather than a $1/\cos\lambda$ latitude dependence. Again, the

Table 2
Averages Values of Solar Wind Parameters for the Peak and Dip Periods

Parameter	Peaks	Dips
V_p	794 ± 2	726 ± 2
$T_pR^{1/2}$	2.24 ± 0.06	.89 ± 0.04
$n_pV_{pR}R^2$	1.40 ± 0.06	1.22 ± 0.03
100 n_a/n_p	4.76 ± 0.08	4.51 ± 0.11
B_RR^2	−1.8 ± 0.1	−2.4 ± 0.2
100 Fe/O	5.9 ± 0.3	4.2 ± 0.3
C^{6+}/C^{5+}	59 ± 7	91 ± 12
100 O^{7+}/O^{6+}	8.3 ± 0.1	9.6 ± 0.2
QFe	10.0 ± 0.1	10.2 ± 0.1

Notes. From top to bottom: V_p = proton speed in km s^{-1}; $T_pR^{1/2}$ = proton kinetic temperature, in 10^6 K, normalized by the square root of the solar distance in AU; $n_pV_{pR}R^2$ = proton flux in units of 10^8 cm^{-3} km s^{-1} normalized by the square of the solar distance in AU; n_a/n_p = the ratio of alpha-particle to proton densities; B_RR^2 = the radial component of the interplanetary field, in nT, normalized by the square of the solar distance in AU; Fe/O = the ratio of the densities of iron to oxygen ions; C^{6+}/C^{5+} = the ratio of the densities of C^{6+} to C^{5+} ions; O^{7+}/O^{6+} = the ratio of densities of O^{7+} to O^{6+} ions; and QFe = the average charge state of iron ions. The uncertainties are standard errors, not standard deviations.

conclusion is that the microstreams are related to episodic rather than quasistationary sources.

Average values of each of several solar-wind parameters were calculated for each Peak and each Dip, and those averages were then averaged over all the Peaks or Dips. Some of the results are presented in Table 2. The velocity correlations of several of the results shown in Table 2 agree with those found in Paper 1 for the previous solar-cycle minimum. Namely, the normalized temperature and the alpha-particle abundance were positively correlated with velocity. In 2007–2008, however, the normalized proton flux was slightly greater for the Peaks than for the Dips. Those parameters not studied before show some interesting differences between the Peaks and Dips. The normalized radial field component, measured by the *Ulysses* magnetometer (Balogh et al. 1992), was weaker in the Peaks than in the Dips; note that the average field was inward, so the Dips had greater negative values. The SWICS instrument (Gloeckler et al. 1992) measured the charge state and elemental compositions of many solar wind ions. Table 2 shows that carbon and oxygen were both less highly ionized in Peaks than in Dips. The enhanced ratio of iron to oxygen in the Peaks is presented in greater detail below.

As discussed in Section 2, X-ray jets are described as having sharp boundaries while plumes are fuzzier without sharp boundaries. Figure 3 illustrates the shapes of the velocity profiles of the 14 Peaks observed through 2008 January 13, when the data coverage was still complete. Each panel is a plot of the velocity profile through a Peak period; note that the timescale, given as day number at the bottom of each panel is not uniform, but varies to fit the data. The dashed lines denote the long-term average speed plus 20 km s^{-1}. Most of the profiles show sharp jumps in velocity, although some, such as panels (e) and (l) are relatively smooth.

The nature of some of the discontinuities in the first Peak (panel (a)) can be understood with the data presented in Figures 4 and 5. The data in those figures are SWOOPS spectrum-by-spectrum determinations of the plasma properties together with magnetometer data acquired at the time of the measurement of the peak of each proton spectrum. The time resolution is 4 minutes, with a few gaps for removal of bad spectra. From top to bottom in Figure 4 are the magnitude of the proton velocity followed by the magnetic pressure (red, on the bottom), the proton thermal pressure (blue, next to bottom), and the sum of the magnetic and proton thermal pressures (green). Figure 5 again shows the proton velocity (this time its principal, radial component) followed by the RTN components of the magnetic field. Vertical lines in Figures 4 and 5 mark the principal discontinuities associated with this Peak.

The first discontinuity in Figures 4 and 5 is clearly a tangential discontinuity separating two plasmas with different properties. While the total pressure remained nearly constant, the magnetic pressure dropped and the proton thermal pressure rose, primarily because of a jump in proton temperature. Many of the discontinuities at the leading edges of the microstream Peaks exhibited such a simultaneous increase in proton temperature and decrease in field strength. The magnetic field rotated through an angle of ∼49° across this discontinuity. There was also a slight decrease in the helium abundance (not shown).

Discontinuity 2 has the properties of a reverse shock propagating into the faster plasma; the velocity increased while the density and field strength dropped.

Discontinuities 3 and 4 both have large changes in the field direction of 102° and 159°, respectively.

Discontinuity 5 marks the end of the velocity Peak. The temperature dropped slightly, the field strength increased, and the helium abundance (not shown) dropped about 30%. The magnetic field rotated through an angle of ∼38°.

How should these discontinuities be interpreted? The fast solar wind is host to many discontinuities, of which only the five largest are noted in Figures 4 and 5. What caused the discontinuities? Were they of solar or interplanetary origin? The reverse shock, #2, was probably generated in the solar wind, not at the Sun. It is suggested that the other four are consistent with the sharp edges of X-ray jets. First, the changes in helium abundance across #1 and #5 were probably of chromospheric or coronal, not interplanetary, origin. Interplanetary turbulence can, however, create magnetic directional discontinuities (e.g., Vasquez et al. 2007; Greco et al. 2009). Borovsky (2008) has studied the frequency of occurrence of discontinuities as a function of the rotation of the magnetic field. He fit the distribution to two exponential functions, with the crossover between large and small rotations at ∼40°. Neugebauer & Giacalone (2010) concluded that most of those with small rotation angles are caused by turbulence while those with large rotation angles originate at the Sun. By that standard, #1, #3, and #4 are probably all of solar origin, while the change in helium abundance adds #5 to that category. If #1 and #5 are the boundaries of the plasma from an X-ray jet, what caused #3 and #4? They could be explained by a second X-ray burst. Madjarska (2011) has identified the triggering of several energy depositions in a single jet. As in coronal mass ejections, later outbursts often have greater speed than their predecessors which have swept out the obstacles to the propagation of the later flows.

Panels (e), (g), and (l) in Figure 3 appear to have slow rises and falls in solar wind velocity together with a superposition of small discontinuities. The Peak in panel (h) exhibits a slow rise, but sharp drop. A possible interpretation is that the Peaks without sharp jumps may be the interplanetary manifestations of wider, fuzzy plumes rather than narrower sharp-edged jets. That suggestion is supported by the time duration of the events in panels (g) and (h); in Figure 2, the three peaks with the longest duration correspond to panels (g), (h), and (n). The longest of

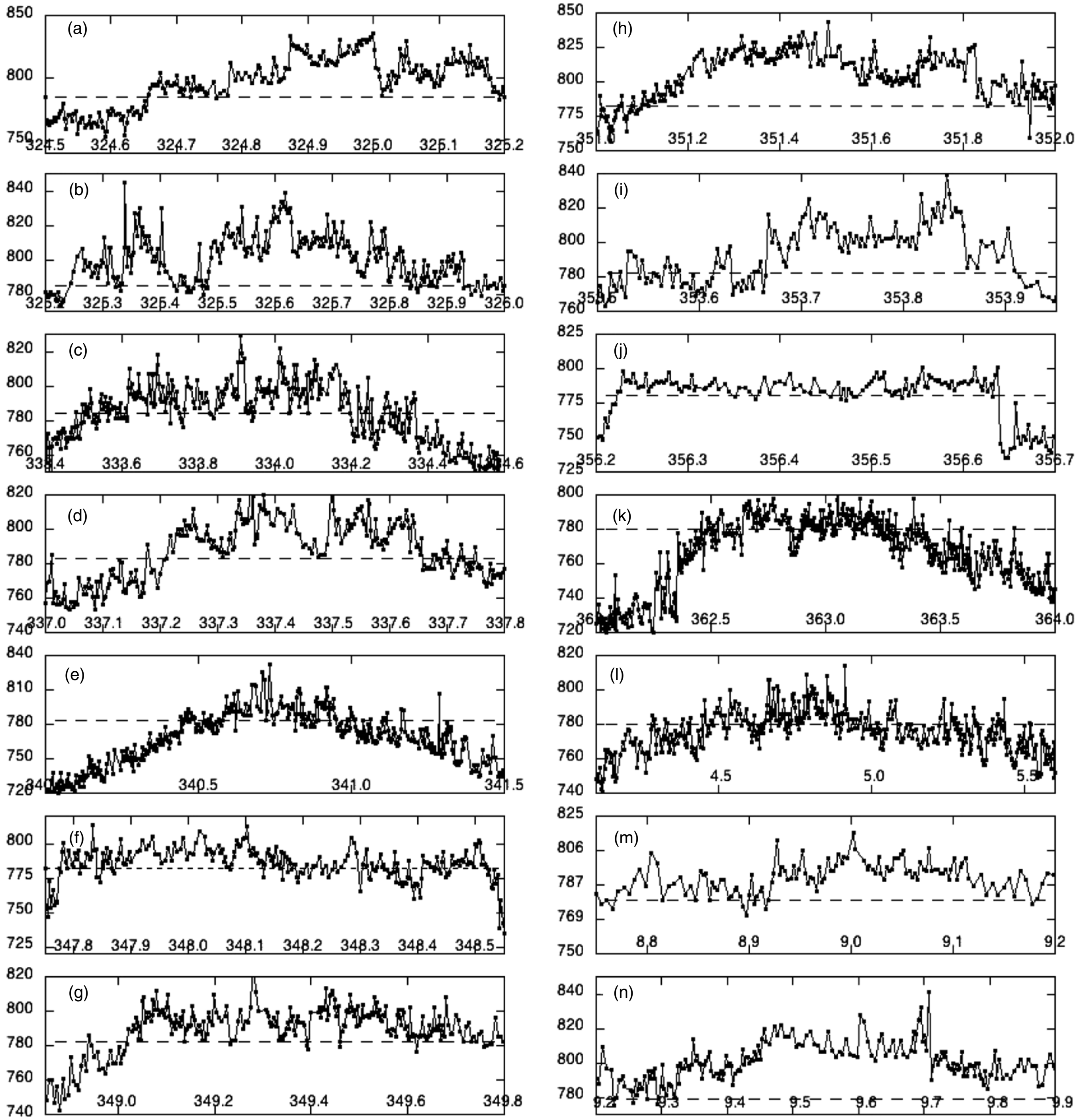

Figure 3. Profiles of velocity variations through 14 microstream Peaks. The units are km s^{-1} (ordinates) and day number (abscissae).

those, panel (n), appears to be a compound event, similar to the structure of the Peak in panel (a).

Figure 6 and Table 2 show a difference in the Fe/O ratio between Peaks and Dips. Relative to the Dips, the Peaks appear to be enhanced in iron, which is an element with a low FIP. This result is surprising in light of the general overall anti-correlation between Fe/O and solar-wind velocity. The slow wind is known to be enriched in low-FIP elements (Geiss et al. 1995). Figure 7 illustrates the dependence of the Fe/O ratio on velocity. Data from the period in early 1993 when *Ulysses* passed in and out of high-speed streams are shown on the left. The top left panel shows speed (in this case of alpha particles as measured by SWICS), while the lower left panel is a scatter plot of three-hour averages of Fe/O versus alpha-particle speed for the same period. The red line is a power-law fit to the data, which has a correlation coefficient of 0.36. Similar plots are shown on the right for the 2007–2008 north polar passage, where the power-law fit is positively correlated with speed. The chi-squared for this fit is 0.51, which implies a 92% chance that the positive correlation is real. (A linear least-squares fit of Fe/O to V gives a correlation coefficient $R = 0.11$, which for the >1000 points in the sample yields a probability of no correlation $P < 0.0004$.)

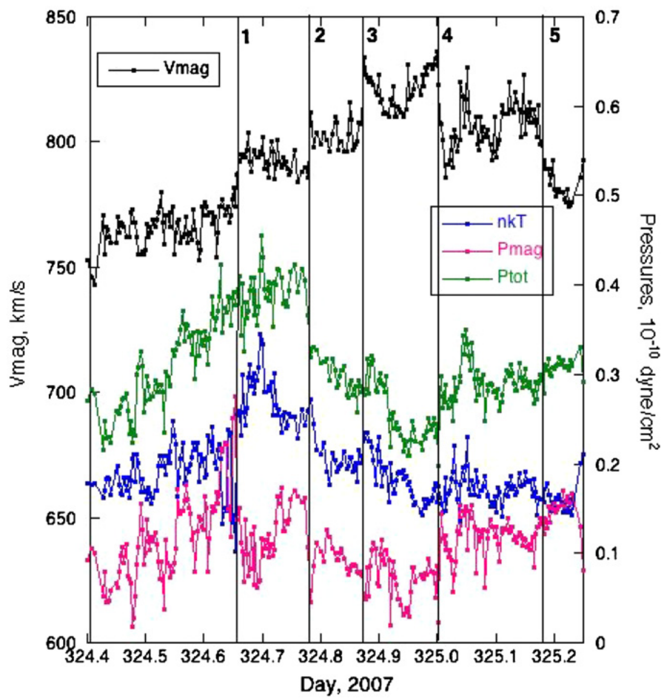

Figure 4. From top to bottom, proton speed (black, in km s^{-1}, scale on the left), sum of the magnetic and proton thermal pressures (green), proton thermal pressure (blue) and magnetic pressure (red). The units for the pressures are 10^{-10} dynes cm^{-2}, given on the right axis. The numbered vertical lines denote specific discontinuities discussed in the text.

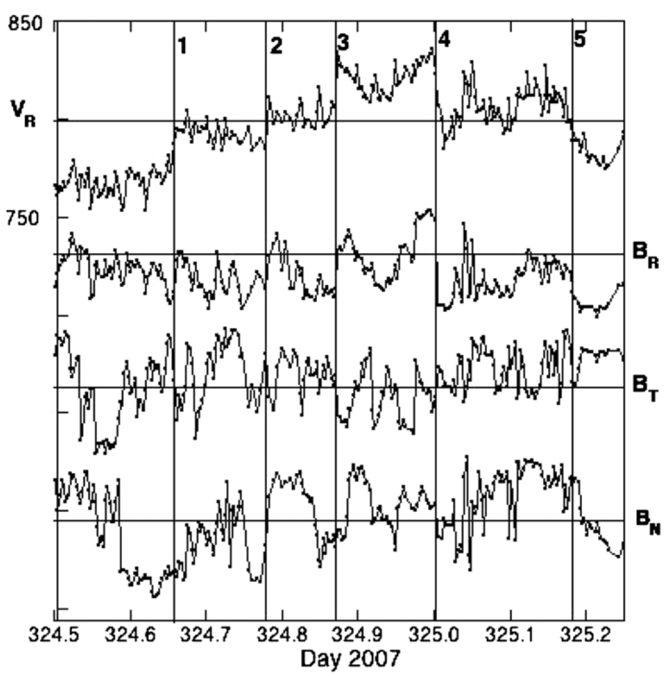

Figure 5. From top to bottom, the radial component of the velocity, in km s^{-1}, and the R, T, and N components of the magnetic field, in nT. The horizontal zero lines for each field component are separated by 4 nT.

The dependence of the Fe/O ratio on speed is evidently double-valued, which is indicated by the parabolic fit shown by the blue curve in the bottom left panel of Figure 7.

4. CONCLUSIONS AND DISCUSSION

It can be concluded from the material presented previously and above that the microstream Peaks in the fast polar solar

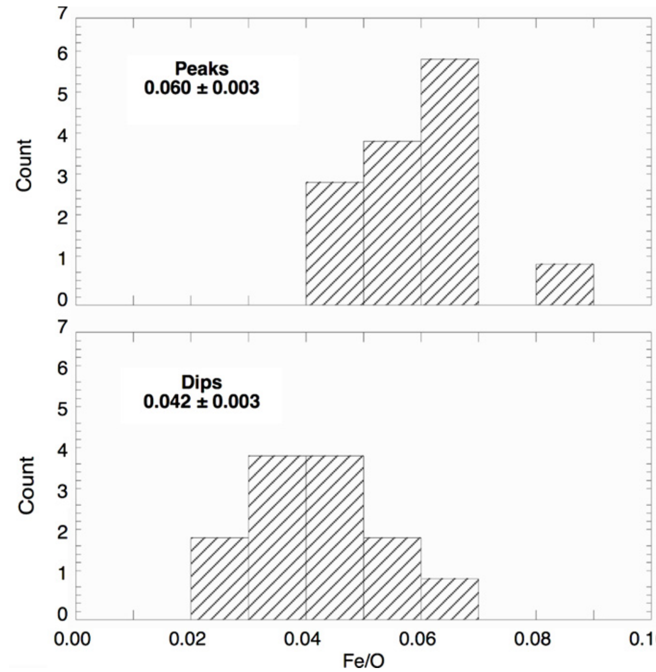

Figure 6. Histograms of the relative densities of iron and oxygen ions for the Peak and Dip periods. The uncertainties are standard errors.

wind during periods of low solar activity are of solar, rather than interplanetary, origin. Both the large-angle discontinuities bounding most of the Peaks and the compositional variations support such a conclusion.

The question then arises, what is the responsible solar feature? In Paper 1, it was argued that both the frequency of occurrence and the lack of a latitude dependence were consistent with an origin in either X-ray jets, or plumes, or the supergranulation boundary, but a choice was not made among those three possibilities. More recent work has shown that the three posited sources are related. Jets arise from magnetic reconnection associated with bright points in supergranulation boundaries and lead to the creation or enhancement of plumes. There is little, if anything, else in the large polar coronal holes that could be the source of the microstream Peaks.

The correlation of the Peaks with increased Fe/O requires some further discussion. The effect shown in Figure 6 is admittedly marginal. The finding of an upturn in Fe/O at the highest speeds (Figure 7) is more robust. A similar upturn at the highest speeds was also found by Wang et al. (2009) using ACE data that included solar-minimum periods when the fraction of open magnetic flux was greatest. On the other hand, Von Steiger et al. (1999) found no such correlation when *Ulysses* was in the fast polar solar wind during the previous solar cycle. Reanalysis of that period in 1994 using the methods of this paper similarly shows no increase of the Fe/O ratio with speed, either in general or in association with microstream Peaks. Thus, a question remains about the persistence of the low-FIP effect in microstreams.

Table 2 shows that the proton temperature and normalized flux were greater in the Peaks than in the Dips, consistent with the temperature, density, and high speeds of hot X-ray jets. Table 2 also shows that the ionization states of carbon and oxygen were lower in the Peaks than in the Dips. Such an inverse correlation of charge state and speed is consistent with the overall behavior of the solar wind. The charge state is determined in the corona at ∼1.3–1.5 solar radii (Ko et al.

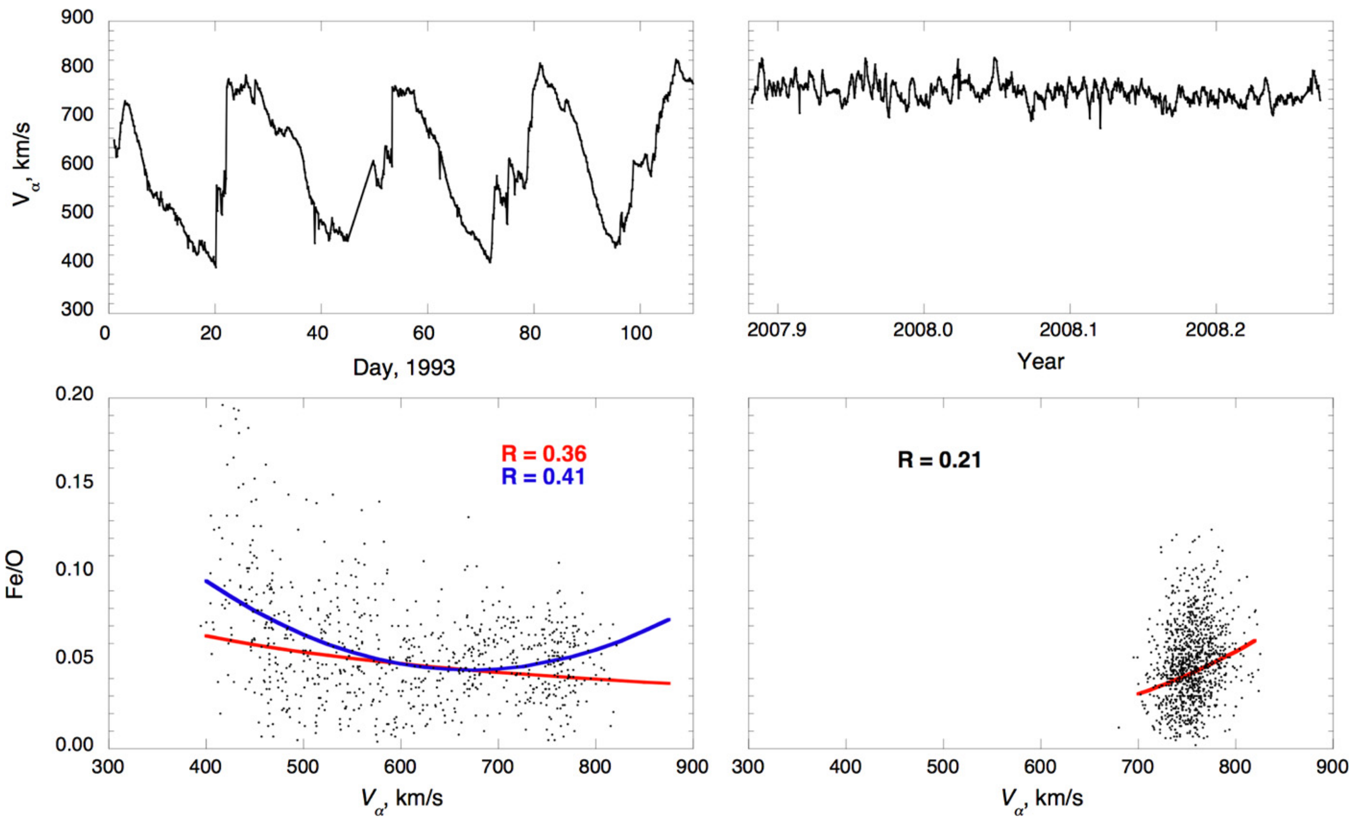

Figure 7. Top: 3 hr averages of alpha-particle velocity vs. time for two different time intervals. Bottom: scatter plot of the Fe/O ratio vs. alpha-particle velocity for the same two intervals. The red lines are least-square fits to power-law relations and the blue curve is a fit to a parabolic relation. *R* is the correlation coefficient.

1997), well above the upper-chromosphere and transition region where the elemental abundance of the solar wind is determined.

It is also noted that Table 2 shows that the normalized radial component of the interplanetary field is weaker in the Peaks than in the Dips. That relation could arise from either, or both, of two processes. First, the eruption of bright-point loops to form jets is a process that converts magnetic energy to kinetic energy. But it should be noted that because the polar magnetic field was oriented inward toward the Sun, any outward propagating Alfvén wave that increased the radial component of the solar-wind velocity would simultaneously decrease the inward radial component of the field. The ubiquity of outwardly propagating Alfvén waves in the high speed wind prevents the separation of those two effects.

The authors of Paper 1 were unable to reach a conclusion about the solar source(s) of the microstreams. Possibilities included coronal jets, coronal plumes, or the supergranulation structure. The properties of the majority of the microstream Peaks shown in this paper, such as the sharp edges and the high temperatures and fluxes, suggest that the peaks are more likely to be associated with jets than with plumes. According to Brueckner & Bartoe's (1983) observations, a large coronal jet could provide more than enough energy to accelerate the plasma in a microstream from 750 to 790 km s^{-1}.

There have been several attempts (Del Zanna et al. 1998; Casalbuoni et al. 1999; Velli et al. 2011) to model the evolution of plume material into the solar wind at or beyond 1 AU, with varying results. The model by Del Zanna et al. (1998) can yield plume plasma at 1 AU with flow velocity greater than that of the surrounding interplume plasma, but other models fail to accelerate the plume material up to the speed of the surrounding solar wind. In the future, such models should include the properties of X-ray jets as boundary conditions.

The data and considerations included in this report lead me to believe that jets, rather than plumes, are the probable cause of most of the microstream Peaks.

This research would not have been possible without the efforts of the people responsible for the design, construction, and operation of the SWOOPS, SWICS, and magnetometer experiments as well as for the *Ulysses* mission as a whole. I thank them all for making their data publicly available. I am also grateful for the helpful thoughts and suggestions of the anonymous referee.

REFERENCES

Balogh, A., Beek, T. J., Forsyth, R. J., et al. 1992, A&AS, 92, 221
Bame, S.J., Asbridge, J. R., Feldman, W. C., & Gosling, J. T. 1977, J. Geophys. Res., 82, 1487
Bame, S.J., McComas, D. J., Barraclough, B. L., et al. 1992, A&AS, 92, 237
Borovsky, J.E. 2008, J. Geophys. Res., 113, A08110
Brueckner, G. E., & Bartoe, J.-D. F. 1983, ApJ, 272, 329
Casalbuoni, S., Del Zanna, L., Habbal, S. R., & Velli, M. 1999, J. Geophys. Res., 104, 9947
Cirtain, J.W., Golub, L., Lundquist, L., et al. 2007, Science, 318, 1580
Cranmer, S. R. 2009, Living Rev. Sol. Phys., 6, 3
Del Zanna, L., Von Steiger, R., & Velli, M. 1998, Space Sci. Rev., 85, 349
Gabriel, A. H., Bely-Dubau, F., & Lemaire, P. 2003, ApJ, 589, 623
Geiss, J., Gloeckler, G., von Steiger, R., et al. 1995, Science, 268, 1033
Gloeckler, G., Geiss, J., Balsiger, H., et al. 1992, A&AS, 92, 267
Gosling, J. T., Riley, P., McComas, D. J., & Pizzo, V. J. 1998, J. Geophys. Res., 103, 1941

Greco, A., Matthaeus, W. H., Servidio, S., Chuychai, P., & Dmitruk, P. 2009, ApJ, 691, L111
Ko, Y.-K., Fisk, L. A., Geiss, J., et al. 1997, Sol. Phys., 171, 345
Madjarska, M. S. 2011, A&A, 526, A19
McComas, D. J., Hoogeveen, G. W., Gosling, J. T., et al. 1996, A&A, 316, 368
Moreno-Insertis, F., Galsgaard, K., & Ugarte-Urra, I. 2008, ApJ, 673, L211
Neugebauer, M., Goldstein, B. E., McComas, D. J., Suess, S. T., & Balogh, A. 1995, J. Geophys. Res., 100, 23389
Neugebauer, M., & Giacalone, J. 2010, in AIP Conf. Proc. 1216, 12th Intl. Solar Wind Conf., ed. M. Maksimovic et al. (Melville, NY: AIP), 194
Raouafi, N.-E., Petrie, G. J. D., Norton, A. A., & Solanki, S. K. 2008, ApJ, 682, 137
Reisenfeld, D. B., McComas, D. J., & Steinberg, J. T. 1999, Geophys. Res. Lett., 26, 1805
Subramanian, S., Madjarska, M. S., & Doyle, J. G. 2010, A&A, 516, A50
Suess, S. T. 1998, Solar Jets and Coronal Plumes (ESA SP-421; Noordwijk: ESA), 223
Thieme, K. M., Marsch, E., & Schwenn, R. 1990, Ann. Geophys., 8, 713
Vasquez, B. J., Abramenko, V. I., Haggerty, D. K., & Smith, C. W. 2007, J. Geophys. Res., 112, A11102
Velli, M., Lionello, R., Linker, J. A., & Mikić, Z. 2011, ApJ, 736, 32
Von Steiger, R., et al. 1999, in AIP Conf. Proc. 471, Solar Wind Nine, ed. S. R. Habbal et al. (Melville, NY: AIP), 143
Wang, X., Klecker, B., & Wurz, P. 2009, A&A, 505, 1237
Wang, Y.-M., Hawley, S. H., & Sheeley, N. R., Jr. 1998, Science, 271, 464
Wilhelm, K. 2006, A&A, 455, 697
Wilhelm, K., Dammasch, I. E., Marsch, E., & Hassler, D. M. 2000, A&A, 353, 749